Anal. Chem. **2005,** *77,* 5542−5550

Quantification of Quaternary Mixtures of Low Alcohols in Water: Temporal-Resolved Measurements with Microporous and Hyperbranched Polymer Sensors for Reduction of Sensor Number

Matthias Vollprecht,[†] Frank Dieterle,[†] Stefan Busche,*[,†] Günter Gauglitz,[†] Klaus-Jochen Eichhorn,[‡] and Brigitte Voit[‡]

Institute of Physical and Theoretical Chemistry, University of Tübingen, Auf der Morgenstelle 8, 72076 Tübingen, Germany, and Institute of Polymer Research Dresden e.V., Hohe Strasse 6, 01069 Dresden, Germany

The focus of this study is the quantification of multianalyte mixtures in water by the use of sensor arrays based on polymer layers. Reflectometric interference spectroscopy is used as a optical sensor system for temporal-resolved measurements of the interaction kinetics of analytes in water with the polymer layers. The principles and widespread possibilities of this approach are demonstrated using the quantification of quaternary aqueous mixtures of low alcohols from methanol up to 1-butanol. The sensitive layers consist of two hyperbranched polyesters and one microporous polyimide. Different time-dependent sensor signals are evaluated by artificial neural networks. Because the kinetics of sorption and desorption of the analytes differ significantly, the number of sensors needed for a quantification of analytes in mixtures can be reduced. A feature extraction allows identification of the most important differences of kinetic patterns of the analytes and allows improvement of the multivariate calibration. It is shown that a quantification of quaternary mixtures of methanol, ethanol, 1-propanol, and 1-butanol is possible on the basis of only two polymer sensors.

The quantification of multianalyte mixtures in gas or liquid phases is of great interest. An efficient protection of air and water requires powerful analytical tools for sites exposed to pollution. For this purpose, most of the common analytical methods require a time- and money-consuming sampling on-site followed by a transfer of the samples to a laboratory. In the past decade, optical sensors have been established as new and useful tools for the real-time detection and quantification of environmentally relevant compounds or of mixtures on-line or even in-line in the environment. These sensing devices enable fast, reproducible, long-term, and inexpensive monitoring. Many of different applications for optical sensors have been reported in the literature.[1,2]

Because a sensory approach is not based on a separation effect, such as GC or HPLC, the quantification of a multianalyte mixture requires a sensor array with polymer films of different sensitivities. For the calibration of such a sensor array, usually only one single property per sensor signal, for example, the area, the slope at a certain time point, or the height at equilibrium, is used for data analysis. By evaluating the sensor response with model-based multivariate methods or artificial neural networks, a qualification and quantification of analytes in mixtures is possible.[3−8] The main drawback of this widespread approach is that the multivariate calibration methods for the quantification of multiple analytes in mixtures need as many sensor signals and sensors as analytes to be quantified; otherwise, the system would be statistically underdetermined. This renders the array approach hardware- and cost-intensive for many applications.

In contrast to such static sensor measurements, a very recent trend in sensor research is the exploitation of the interaction kinetics of a sensor with different analytes by the use of temporal-resolved measurements. If various analytes of a mixture show different kinetics for the sorption into sensitive polymer layers due to different size or polarity of these analytes, the resulting sensor response differs in shape for all analytes. If such sensors are combined with multivariate data analysis techniques, such as artificial neural networks, the number of analytes quantified per sensor is limited only by the similarity of interaction kinetics. A virtual sensor array is created, and the number of sensors necessary for the quantification can be reduced.

The investigation of such temporal-resolved approaches in gas and liquid phases have been reported by several groups.[9−13] By temporal-resolved measurements with an array of quartz microbal-

* Corresponding author. Phone: +49 (0) 7071/29-78760. Fax: +49 (0) 7071/29-5960. E-mail: stefan.busche@ipc.uni-tuebingen.de.

[†] University of Tübingen.

[‡] Institute of Polymer Research Dresden e.V.

(1) Janata, J.; Josowicz, M. *Anal. Chem.* **1998**, *70*, 179−208.

(2) Wolfbeis, O. S. *Anal. Chem.* **2002**, *74*, 2663−2678.

(3) Doleman, B. J.; Lonergan, M. C.; Severin, E. J.; Vaid, T. P.; Lewis, N. S. *Anal. Chem.* **1998**, *70*, 4177−4190.

(4) Park, J.; Groves, W. A.; Zellers, E. T. *Anal. Chem.* **1999**, *71*, 3877−3886.

(5) Seemann, J.; Rapp, F. R.; Zell, A.; Gauglitz, G. *Fresenius' J. Anal. Chem.* **1997**, *359*, 100−106.

(6) Schaffer, R. E.; Rose-Pehrsson, S. L.; McGill, R. A. *Anal. Chim. Acta* **1999**, *384*, 305−317.

(7) Hierlemann, A.; Weimar, U.; Kraus, G.; Gauglitz, G.; Göpel, W. *Sens. Mater.* **1995**, *7*, 179−189.

(8) Grate, Y. W.; Wise, B. M. *Anal. Chem.* **2001**, *73*, 2239−2344.

10.1021/ac0504316 CCC: $30.25
Published on Web 08/09/2005

ances coated with three different polymer films, six solvent vapors could be classified.[14] Even single-sensor approaches in the gas phase have been performed. The quantification of a binary mixture of alcohols or refrigerants was performed by the use of a surface plasmon resonance (SPR) device on the basis of measurements in a temporal-resolved mode.[15,16] Two single-sensor setups for the quantification of quaternary mixtures of alcohols in the gas phase were reported by Kasper et al.[17] Binary and ternary mixtures of organic analytes in water were determined by one single amperometric sensor.[18,19] A static reflectometric interference sensor was used for the quantification of binary mixtures of low alcohols in water.[20] So far, no temporal-resolved measurements have been performed in the liquid phase on the basis of polymer sensors.

In this study, the simultaneous quantification of methanol, ethanol, 1-propanol, and 1-butanol in a quaternary mixture in water is presented. The homologous alcohols were chosen as an inexpensive model system, which is soluble in water, nontoxic, and easily disposable. Their sizes are on the same order of dimension as the pores of the microporous polymer used: methanol is smaller (0.068 nm^3), ethanol is about the same size (0.097 nm^3), and *n*-propanol (0.125 nm^3) as well as *n*-butanol (0.152 nm^3) is bigger than the mean pore volume of the microporous polymer (0.118 nm^3). Temporal-resolved measurements of pure analytes and mixtures were performed by reflectometric interference spectroscopy (RIfS) using a polymer sensor array consisting of three different polymer sensors. A polyimide sensor was used as a microporous polymer especially for the quantification of smaller-sized analytes. Polyimide films are applied in microelectronics and microelectromechanical systems technology. Sensory applications of polyimides were presented in refs 21 and 22. Until now, polyimide sensors have been applied neither for temporal-resolved measurements nor for the quantification of multianalyte mixtures. Additionally, two different hyperbranched polyester sensors were used in the sensor array. Recently, hyperbranched polymers have received much attention due to their unique chemical and physical properties.[23] The highly branched structure and end group functionality of the hyperbranched polymers result in very low solution viscosity; strongly improved solubility in a wide variety of solvents; fully amorphous structure; high compatibility with other polymers; and much stronger interactions with solvents, organic molecules, and other polymers in general. The thermal, mechanical, and the dynamic properties of the polymers are governed mainly by the nature of the end groups and not by the structure of the repeating units of the backbone. An overview of different applications of such polymer systems has been given by Gao and Yan.[24] The suitability of hyperbranched polymers for gas and solution separations is presented in several publications.[25–27] A polymeric "molecular filter" for chemical sensors consisting of hyperbranched films and β-cyclodextrin receptors was reported by Dermody et al.[28] Hyperbranched polyesters have been formerly applied as sensor materials for the quantification of single analytes in the gas phase.[29]

In this work, it is shown that the combination of one or two hyperbranched polymers as sensitive layers, one microporous polymer as sensitive layer, temporal-resolved measurements, and multivariate data analysis allow quantifications of quaternary mixtures of alcohols in water within a broad concentration range.

EXPERIMENTAL SECTION

Reflectometric Interference Spectroscopy. Reflectometric interference spectroscopy (RIfS) is based on the multiple reflectance of white light at a layer system. The parts of the light reflected at different interfaces of the layer system superimpose and form an interference pattern. This interference pattern depends on the optical thickness of the layer, which is given by the product of refractive index and physical thickness. One part of the radiation is reflected at the interface of a thin layer, whereas the other part penetrates the layer and is reflected at the other interface. These two partial reflected beams superimpose and form an interference pattern, resulting in constructive or destructive interference. A reversible swelling of the polymer film is correlated with changes in optical thickness. The setup has been described in detail elsewhere.[30] Briefly, the setup consists of a tungsten light source, optical Y-fiber couplers (PMAA, 1-mm core diameter, microparts, Dortmund, Germany) and a diode array spectrometer (MMS, Zeiss, Jena, Germany). The temperature of the flow cell is kept constant by a thermoregulator.

Polymer Materials. Three different polymer systems were used as sensitive sensor layers. The chemical structures of these polymer systems are shown in Figure 1. The commercial polyimide system PI 2566 (a) features a microporous structure with a mean pore volume of 0.118 nm^3. The chemical properties of this polymer system are dominated by a high glass transition temperature (T_g = 290 °C) resulting in a high density and hardness.[16] The two hyperbranched polyesters (HBPs) vary in their chemical properties due to different functional groups (hydroxy groups and acetate groups), different molar weights, and different glass transition temperatures. Details about synthesis and properties

(9) White, J.; Kauer, J. S.; Dickinson, T. A.; Walt, D. *Anal. Chem.* **1996**, *68*, 2191−2202.
(10) Sutter, J. M.; Jurs, P. C. *Anal. Chem.* **1997**, *69*, 856−862.
(11) Johnson, S. R.; Sutter, J. M.; Egelhardt, H. L.; Jurs, P. C.; White, J.; Kauer, J. S.; Dickinson, T. A.; Walt, D. R. *Anal. Chem.* **1997**, *69*, 4641−4648.
(12) Kieser, B.; Dieterle, F.; Gauglitz, G. *Anal. Chem.* **2002**, *74*, 4781−4787.
(13) Busche, S.; Dieterle, F.; Kieser, B.; Gauglitz, G. *Sens. Actuators, B* **2003**, *89*, 192−198.
(14) Sugimoto, I.; Nakamura, M.; Kuwano, H. *Sens. Actuators, B* **1993**, *10*, 117−122.
(15) Dieterle, F.; Busche, S.; Gauglitz, G. *Anal. Chim. Acta* **2003**, *490*, 71−83.
(16) Kieser, B.; Dieterle, F.; Gauglitz, G. *Anal. Chem.* **2002**, *74*, 4781−4787.
(17) Kasper, M.; Busche, S.; Dieterle, F.; Belge, G.; Gauglitz, G. *Meas. Sci. Technol.* **2004**, *15*, 540−548.
(18) Slama, M.; Zabrosch, C.; Wienke, D.; Spener, F. *Anal. Chem.* **1996**, *68*, 3845−3850.
(19) Plegge, V.; Slama, M.; Süselbeck, B.; Wienke, D.; Spenke, F.; Knoll, M.; Zabrosch, C. *Anal. Chem.* **2000**, *72*, 2937−2942.
(20) Dieterle, F.; Nopper, D.; Gauglitz, G. *Fresenius' J. Anal. Chem.* **2001**, *370* (6), 723−730.
(21) Buchhold, R.; Nakladal, A.; Gerlach, G.; Sahre, K.; Müller, M.; Eichhorn, K.-J.; Herold, M.; Gauglitz, G. *J. Electrochem. Soc.* **1998**, *145*, 4012−4018.
(22) Wessa, T.; Barie, N.; Rapp, M.; Ache, H. J. *Sens. Actuators, B* **1998**, *53*, 63−68.
(23) Voit, B. J. *Polym. Sci.: Part A., Polym. Chem*. **2005**, *43*, 2679−2699.
(24) Gao, C.; Yan, D. *Prog. Polym. Sci.* **2004**, *29*, 183−275.
(25) Fang, J.; Kita, H.; Okamoto, K. I. *J. Membr. Sci.* **2001**, *182*, 245−256.
(26) Seiler, M.; Arlt, W.; Kautz, H.; Frey, H. *Fluid Phase Equilib.* **2002**, *201*, 359−379.
(27) Seiler, M.; Köhler, D.; Arlt, W. *Sep. Purif. Technol.* **2002**, *29*, 245−263.
(28) Dermody, D.; Peez, R.; Bergbreiter, D.; Crooks, R. *Langmuir* **1999**, *15*, 885−890.
(29) Belge, G.; Beyerlein, D.; Betsch, C.; Eichhorn, K.-J.; Gauglitz, G.; Grundke, K.; Voit, B. *Anal. Bioanal. Chem.* **2002**, *374*, 403−411.
(30) Brecht, A.; Gauglitz, G.; Kraus, G.; Nahm, W. *Sens. Actuator, B* **1993**, *11*, 21−27.

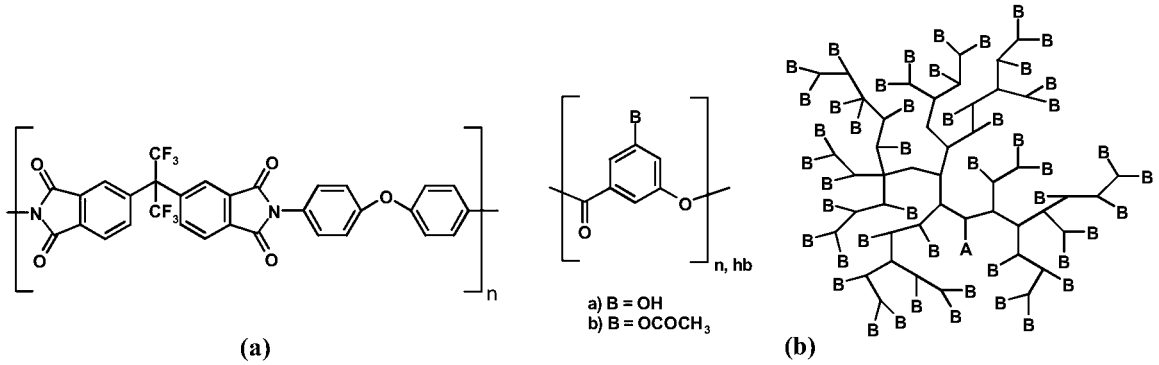

Figure 1. Polyimide PI 2566 (a) and hyperbranched polyester with different functional groups (b).

of these HBPs can be found in refs 31−33. HBP−OAc with an acetic acid moiety to a phenol hydroxyl group can be hydrolyzed slowly in humid air during a long time of storage (several months). This reaction can be accelerated in aqueous solution under basic conditions; however, our solutions with the largest concentration of alcohols (16 000 ppm) have pH values between 5.5 and 6.0. Therefore, a hydrolysis of the HBP−OAc did not occur at room temperature within the applied exposition time.

Coating Procedures. The glass substrates (D 263 with 45 nm Ta_2O_5 and 20 nm SiO_2, Schott, Mainz, Germany) were cleaned and activated with a mixture of hydrogen peroxide and concentrated sulfuric acid (1:2) in an ultrasonic bath. To increase the stability of the polymer films on the substrate, an amino-terminated silane (Pyralin VM-651, HD MicroSystems, Bad Homburg, Germany) was used as adhesions promoter. A 10-μL portion of Pyralin was dissolved in a mixture of 9.5 mL of methanol and 0.5 mL of deionized water and was kept overnight at room temperature. Afterward, a 20-μL aliquot of the solution was dropped onto the substrate, left for 20 s, and spin-coated (Convac 2001, Wiernsheim, Germany) for 30 s at 2000 rpm. The substrate was immediately deposited on a heating surface and was kept for 30 s at 100 °C. Then the different polymers were coated on the hot substrates.

The HBP layers were prepared by spin-coating (60 s at 5000 rpm) a 40-μL aliquot of a 15% w/w (HBP−OH) and 10% w/w (HBP−OAc) solution of the polymer in toluene. Afterward, most of the solvent was removed in an annealing step at 100 °C for 60 s. For the preparation of the polyimide layers (PI 2566, HD MicroSystems, Bad Homburg, Germany), a 40-μL aliquot of a 5% w/w solution of the polyamide acid in *N*-methyl-2-pyrrolidone was used for the spin-coating step (60 s at 6000 rpm). During an annealing procedure at 400 °C for 1 h, this precursor was converted into the polyimide structure.

The thicknesses of the polymer films were ~500 nm, determined by an alpha-step setup (Tencor Instruments, San Jose, CA).

Data Sets. First, single-analyte measurements of methanol, ethanol, 1-propanol, and 1-butanol were performed to characterize the sorption and desorption kinetics of the four different alcohols with the three polymer films. Therefore, the polymer layers were exposed to nine different concentrations of these alcohols between 0 and 16 000 ppm, each for 22 min, and afterward to pure water for 22 min for recovery. Thereby, a spectrum was recorded every 20 s.

In addition to single-analyte measurements, two multicomponent data sets were recorded for the multicomponent analysis of quaternary mixtures. The first data set was a 4-level full factorial design whereby the relative concentrations of the four analytes were varied equidistantly between 0 and 15 000 ppm. This data set was used for the training of the neural networks and for the variable selection and will be hereafter referred to as the calibration data set. The second data set was a 3-level full factorial design with the concentrations equidistantly varied between 2500 and 12 500 ppm. This data set, which will be hereafter referred to as the validation data set, was not involved in the calibration and variable selection but was used for the validation of the final models. All concentration levels of the two data sets differed at the highest possible distance. Thus, the validation data set should give a realistic estimate of the network performance in a real world situation.[34] In total, 256 different mixtures of the four alcohols were measured for the calibration data set, and 81 mixtures were measured for the validation data set. All measurements were performed in triplicate and in random order.

The sensitive layers were exposed to the mixtures for 22 min and afterward to pure water for 22 min for recovery. During the sorption and desorption process, the signal of each sensor was recorded with a resolution of 78 data points, resulting in a total number of 234 data points for all three sensors. These data points were used as independent variables for a multivariate calibration. All data were centered by subtracting the means of the corresponding independent variables. A subsequent division by the standard deviations of the variables standardized the data sets. The concentrations (dependent variables) were range-scaled between −0.9 and 0.9 for processing by neural networks.

Artificial Neural Networks and Variable Selection. The artificial neural networks implemented for this study belong to the class of multilayer feedforward back-propagation networks. Because there are numerous excellent textbooks which describe these types of neural networks in detail,[35−38] only a short outline of the neural networks implemented for this study will be given.

Separate nets were used for each analyte. The topology consisted of one output unit, five hidden units, and as many input

(31) Schmaljohann, D. *Funktionalisierung von hochverzweigten Polyestern für den Einsatz als Beschichtungs- und Blendmaterial*; Herbert Utz Verlag: München; 2001.

(32) Beyerlein, D. *Hochverzweigte Polyester in dünnen Schichten − Charakterisierung der Material- und Grenzflächeneigenschaften*; Tenea Verlag: Berlin; 2002.

(33) Mikhailova, Y.; Pigorsch, E.; Grundke, K.; Eichhorn, K.-J.; Voit, B. *Macromol. Symp.* **2004**, *210*, 271−280.

(34) Jurs, P. C.; Bakken, G. A.; McClelland, H. E. *Chem. Rev.* **2000**, *100*, 2649−2678.

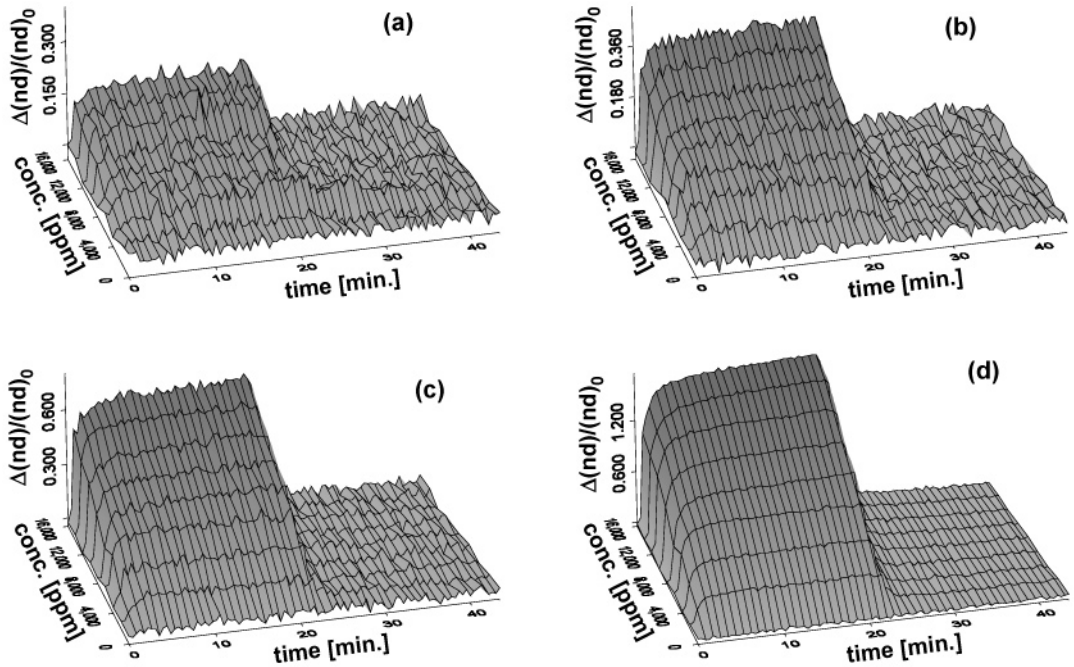

Figure 2. Swelling behavior of HBP−OH for methanol (a), ethanol (b), 1-propanol (c), and 1-butanol (d). The sensor responses are plotted versus time (*x* axis) and concentration of the analyte (*y* axis).

units as time points used. The nets were fully connected. A hyperbolic tangent was used as the activation function for the hidden layer, and a linear activation function was used for the output layer. The training included a maximum of 500 learn cycles. To prevent an overtraining of the neural networks, which means that a neural net learns an often too small calibration data set by heart instead of generalizing the data,[39] an early stopping procedure was used in this study.[40] Thereby, the training is stopped when the error of cross-validation of the calibration data starts to increase, because the net may start losing its generalization ability at this moment. An advanced variant of backpropagation was used as the training algorithm, which is called scaled conjugate gradient (SCG)[41] and which makes use of the pseudo-second-derivative information. In contrast to standard backpropagation, SCG converges faster, is more capable of dealing with local minima, and is not too sensitive to any parameters, which were all set to standard values suggested by Moller.[41]

For the variable selection, a procedure was used, which is described in detail elsewhere.[42] Briefly, this variable selection is based on growing neural networks, according to Vinod et al.[43] The procedure starts with an empty network and inserts different network elements (neurons with one input link and one output link, neurons with two input links and one output link and pure links) to reduce the error of prediction until the improvement of the prediction error is <5%. This procedure is repeated 50 times for each analyte with different partitioning of the calibration data set into calibration and prediction data subsets. Then the variables are ranked according to the frequency of usage in these 200 networks. Finally, the variables are iteratively added to a final neural network in the order of the ranking until a minimum of the error of prediction is reached. Thereby the error of prediction is also calculated as a mean error of 4 × 10 networks with different partitioning of the calibration data into calibration and prediction subsets.

In this study, the quality of prediction of all data is judged using the relative root-mean-square error of prediction.

$$\mathrm{RMSE_{rel}} = \sqrt{\frac{\sum_{i=1}^{N} (\hat{y}_i - y_i)^2}{N}} \Big/ \frac{\sum_{i=1}^{N} y_i}{N} \qquad (1)$$

Thereby, N is the total number of data, $\hat{y}_i$ is the predicted concentration and y_i is the true concentration.

All calculations were performed by a new implementation of the Stuttgart Neural Network Simulator[44,45] on a personal computer.

RESULTS

Single Analytes. For the single analyte measurements, the relative changes in optical thickness plotted versus time and different alcohol concentrations are shown in Figures 2−4 (one

(35) Patterson, D. *Artificial Neural Networks, Theory and Applications*; Prentice Hall Inc: Upper Saddle River, NJ; 1996.
(36) Kaykin, S. *Neural Networks, A Comprehensive Foundation*; Prentice Hall Inc: Upper Saddle River, NJ; 1999.
(37) Zupan, J.; Gasteiger, *J. Neural Networks in Chemistry and Drug Design*, 2nd ed.; Wiley-VCH: Weinheim; 1999.
(38) Principe, J.; Euliano, N.; Lefebvre, W. *Neural and Adaptive Systems: Fundamentals through Simulations*; John Wiley & Sons, Inc.: New York; 2000.
(39) Weigend, A. *Proceedings of the 1993 Connectionist Models Summer School* **1994**, 335−342.
(40) Sarle, W. S. *Proc. 27th Symp. Interface Comput. Sci. Stat.* **1995**, 352−360.
(41) Moller, M. F. *Neural Networks* **1993**, *6*, 525−533.
(42) Dieterle, F.; Busche, S.; Gauglitz, G. *Anal. Chim. Acta* **2003**, *490*, 71−83.
(43) Vinod, V. V.; Ghose, S. *Neurocomputing* **1996**, *10*, 55−69.
(44) Zell, A. *SNNS Stuttgart Neural Network Simulator*; http://www-ra.informatik.uni-tuebingen.de/SNNS/; 2002.
(45) Seemann, J.; Rapp, F. R.; Zell, A.; Gauglitz, G. *Fresenius' J. Anal. Chem.* **1997**, *359*, 100−106.

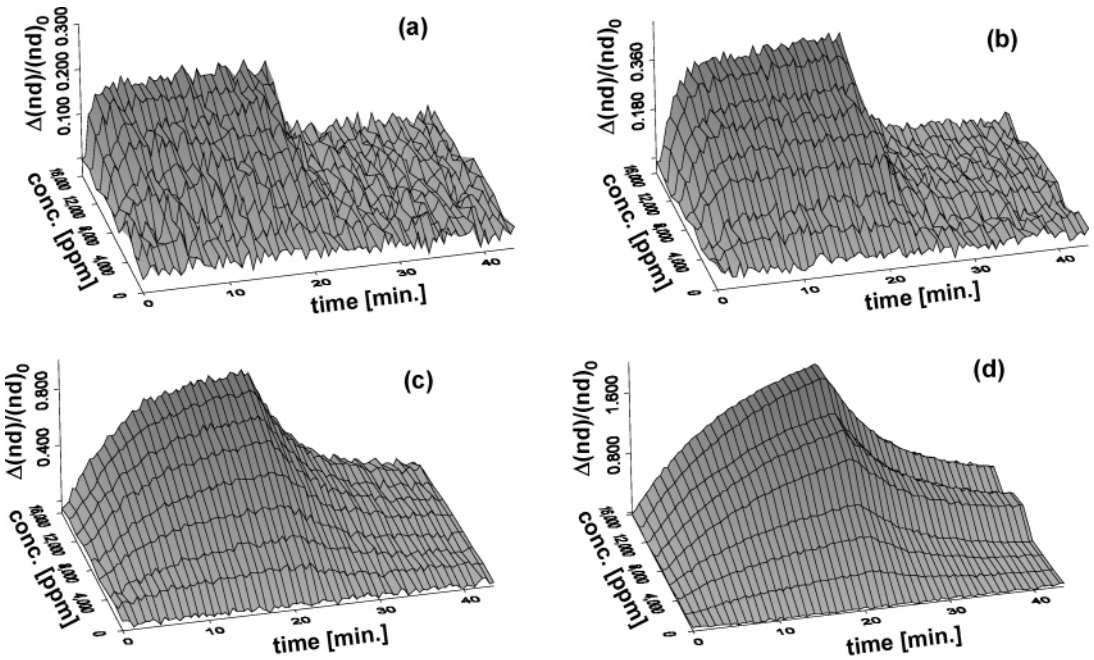

Figure 3. Swelling behavior of HBP−OAc for methanol (a), ethanol (b), 1-propanol (c), and 1-butanol (d). The sensor responses are plotted versus time (*x* axis) and concentration of the analyte (*y* axis). For 1-propanol and 1-butanol, nonlinearities of the sensor responses along the concentration axis and the time axis can be seen.

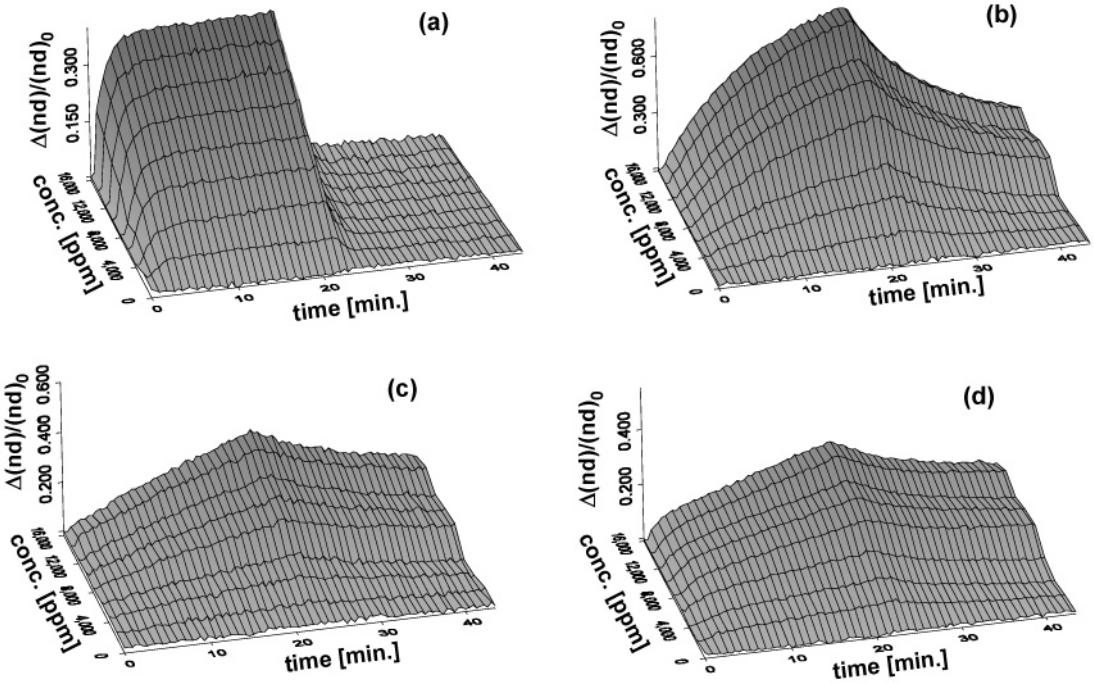

Figure 4. Swelling behavior of PI 2566 for methanol (a), ethanol (b), 1-propanol (c), and 1-butanol (d). The sensor responses are plotted versus time (*x* axis) and concentration of the analyte (*y* axis). For ethanol, nonlinearities of the sensor responses along the concentration axis can be seen.

plot per sensitive layer). The HBP−OH layer shows a similar swelling and deswelling behavior for all four alcohols caused by rather fast interaction kinetics (Figure 2). Thus, for all analytes, the equilibrium state was reached within a few seconds. After the analyte exposition, a complete recovery was observed. Only the height of the sensor signals increased from methanol to 1-butanol. Different swelling and deswelling behavior of the HBP−OAc layer by interaction with the four alcohols was observed (Figure 3). In this case, only for the two smaller alcohols, methanol and ethanol, were fast interaction kinetics observed, resulting in equilibrium states within a few seconds. The resulting signal shape by interaction of the HBP−OAc layer with 1-propanol and 1-butanol indicates a slower sorption and desorption of these alcohols into the polymer. For 1-propanol, the equilibrium state is nearly achieved at the end of analyte exposition, whereas for the homologue 1-butanol, neither the equilibrium state nor a complete recovery was achieved within the measurement period. The signal height increased from methanol up to 1-butanol, despite the slower

Table 1. Relative Root Mean Square Errors (RMSE) for the Predictions of the validation data

method	methanol, %	ethanol, %	1-propano, %	1-butanol, %	mean, %
3 static sensors	55.7	27.9	47.6	23.6	38.7
all variables	24.3	28.3	34.3	24.8	27.9
15 variables	14.4	17.1	30.8	20.3	20.6
single-sensor HBP−OH	53.2	52.9	49.3	29.5	46.2
single-sensor HBP−OAc	32.3	28.8	31.1	21.9	28.5
single-sensor PI 2566	15.9	21.9	44.7	37.2	29.9
2 sensors (HBP−OAc + PI)	14.1	19.1	30.0	22.8	21.5

interaction kinetics that was found for the higher homologues. In comparison, both HBP-systems showed similar signal heights at the end of analyte exposition for the same alcohols, but different interaction kinetics.

For both HBP systems, the differences in swelling and deswelling behavior are influenced on one hand by different functional groups. Small modifications of functional groups and macromolecular architecture of the hyperbranched polymers have a strong effect on the patterns of interaction kinetics of molecules. In the gas phase, a correlation between the polarity of an analyte and the swelling behavior of hyperbranched polyesters with different functional groups was found.[29] Within those investigations, the lower alcohols of higher polarity induced the highest sensor signals. When considering the influence of functional groups on the swelling behavior in aqueous phases, it is important that in aqueous phases the polymer layers are differently swollen due to the uptake of water molecules. A hydration layer surrounds the functional groups and isolates them from a direct interaction with the analytes. Only for the internal accessibility do the functional groups play a crucial role. The branching degree and the macromolecular architecture with various possibilities of hydrogen bonding influence the kinetics of analyte uptake. The slower kinetics of HBP−OAc by interaction with 1-propanol and 1-butanol indicates a more compact macromolecular architecture of higher density.

The swelling and deswelling behavior of the polyimide layer is shown in Figure 4. By interaction with the smallest analyte, fast kinetics was found, and the equilibrium state was achieved within a few seconds. For all three bigger alcohols, a much slower interaction of the polymer film was observed, which is extremely marked for 1-propanol and 1-butanol. By interaction of the PI-2566 layer with ethanol, 1-propanol, and 1-butanol, neither the equilibrium state nor the state of complete recovery is achieved. Although for both HBP systems an increase of signal heights from methanol up to 1-butanol was found, the highest signal for the polyimide layer was recorded by interaction with ethanol, followed by methanol, whereas the interaction with the two biggest alcohols, 1-propanol and 1-butanol, results in the lowest signal heights. The interaction kinetics of analytes of different sizes can be ascribed to the microporous polymer structure. Because methanol is smaller than the mean pore volume of PI 2566, the interaction kinetics of this alcohol is very fast. Ethanol is about the same size or even smaller than the micropores of the polyimide structure. 1-propanol and 1-butanol are bigger than the mean pore volume of the polyimide structure. As expected, the interaction kinetics of these two alcohols is very slow. The differences in swelling and deswelling behavior of the polyimide sensor are directly correlated with the molecular size of the alcohols.

As a result of the single analyte measurements, it can be concluded that the combination of the three sensitive layers should allow the quantification of multianalyte mixtures by temporal-resolved sensor measurements.

Mixtures. On the basis of the different interaction kinetics, which were found for the three polymer films by interaction with single analytes, the data analysis of measurements of quaternary mixtures of the four homologue alcohols methanol, ethanol, 1-propanol, and 1-butanol was carried out by the use of artificial neural networks. If only one single property per sensor signal is extracted and used for the training of the neural networks, the quantification of four analytes by three variables with no constraints of the concentrations is mathematically underdetermined. To simulate these static sensor measurements, the heights of the signals of all three sensors just before the end of exposure to the analyte were used for data analysis. The results of the three static sensors are presented in Table 1. It can be seen that the quantification is very poor. By taking advantage of the dynamic interaction kinetics, better results can be obtained. A neural network using all 234 time points of all three sensors was trained with the calibration data set. The validation data set was used to test the performance of the network. In Table 1, the relative RMSEs are shown. The predictions of methanol and 1-butanol show about the same error, whereas the highest error was obtained for the prediction of 1-propanol. For ethanol, intermediate errors of prediction were obtained.

The quality of this prediction of the networks using all 234 time points can be improved because the high number of 234 input variables results in a high number of 1181 adjustable parameters of the neural networks. This prevents iterative calibration methods, such as the training of neural networks from finding optimal models[46] ending up in a rather poor local training minimum. The number of variables exceeds the number of measurements, causing the problem of overtraining,[47,48] even if an early stopping procedure is used. Among the 234 variables, much information is redundant, noisy, or irrelevant for the training of the neural networks.[49]

A variable selection was performed on the basis of growing neural networks, resulting in an optimal subset of variables. The feature extraction selected 15 time points out of 234, whereby all

(46) Broadhurst, D.; Goodacre, R.; Jones, A.; Rowland, J. J.; Kell, D. B. *Anal. Chim. Acta* **1997**, *348*, 71−86.
(47) Martens, H.; Naes, T. *Multivariate Calibration*; John Wiley & Sons Inc.: New York; 1989.
(48) Richards, E.; Bessant, C.; Saini, S. *Chemom. Intell. Lab. Syst.* **2002**, *61*, 35−49.

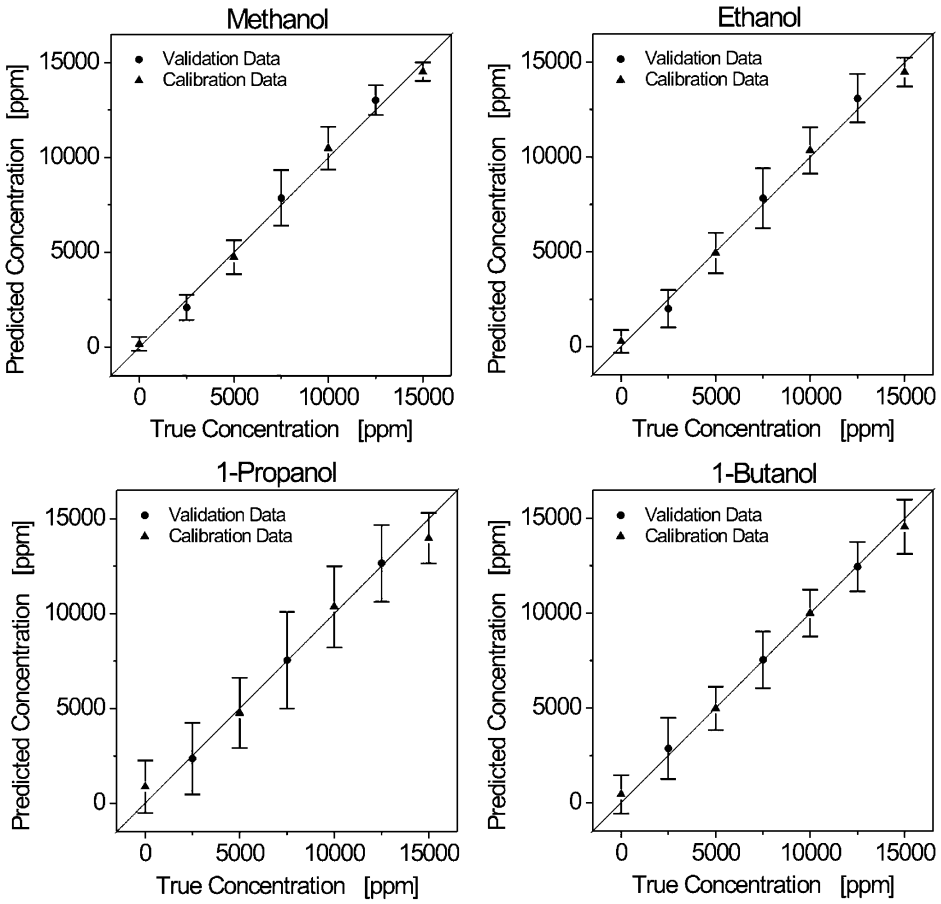

Figure 5. True-predicted plots for the predictions by the networks, which use 15 variables selected by the variable selection process.

three polymers were represented. The predictions of the validation data by the network, which uses these 15 input variables and which was trained by the calibration data set, are better than the predictions of the network using all variables. The relative RMSE for the prediction of the single alcohols as well as the mean of the relative RMSE for all four analytes is lower. It is noteworthy that the decrease of the prediction error for the two lower alcohols is higher than for 1-propanol and 1-butanol.

The predictions of the calibration and validation data using the optimized network with 15 input variables are shown in Figure 5 as so-called true-predicted plots. The true concentrations are plotted versus the predicted concentrations. Because the single data points cannot be graphically resolved, the predictions of each concentration level are represented by the mean and the standard deviation. It is visible that the predictions of all concentration levels are not biased. The predictions of the validation data are only slightly more scattered than the predictions of the calibration data (the scattering is represented by the standard deviation). This indicates a good generalization ability of the neural networks using only 15 variables. In addition, a limit of detection of the four analytes can be approximated by[50]

$$L_D = 2t_{1-\alpha,\nu}s_0 \qquad (2)$$

Thereby L_D is the limit of detection, s_0 is the standard deviation for the concentration "0" of the corresponding analyte, and t represents the one-sided critical values of the Student's t-test whereby α was set to 0.05 and ν represents the degrees of freedom. Both the standard deviation and the degrees of freedom were derived from that part of the full factorial design of the calibration data, for which the corresponding analyte was 0 and for which all other analytes were varying. The limit of detection is 1197 ppm for methanol, 2017 ppm for ethanol, 4618 ppm for 1-propanol, and 3369 ppm for 1-butanol. At first glance, these limits of detection seem to be very high; however, it has to be noted that these values were calculated for mixtures, in which three other cross-reactive analytes were highly varying. Many estimations of limits of detections reported in the literature are based on single-analyte measurements, not on measurements in mixtures. In addition, both the sensor setup and the experimental design were not optimized for measurements of low concentrations of analytes but for measurements of mixtures with a broad range of concentrations.

The variable selection procedure not only selects the most important variables, but also gives an impression of the importance of all variables. In Figure 6, the importance of all time points of the three sensors is plotted as the frequency of selection of the variable selection procedure. The 15 most important variables marked as black bars in Figure 6 were used for the optimized networks, as described before. It is obvious that for all three sensors, similar time intervals are most important for a successful multianalyte determination. Mainly sensor signals at the beginning

(49) Seasholtz, M. B.; Kowalski, B. *Anal. Chim. Acta* **1993**, *277*, 165−177.
(50) Currie, L. A. *Chemom. Intell. Lab. Syst.* **1997**, *37*, 151−181.

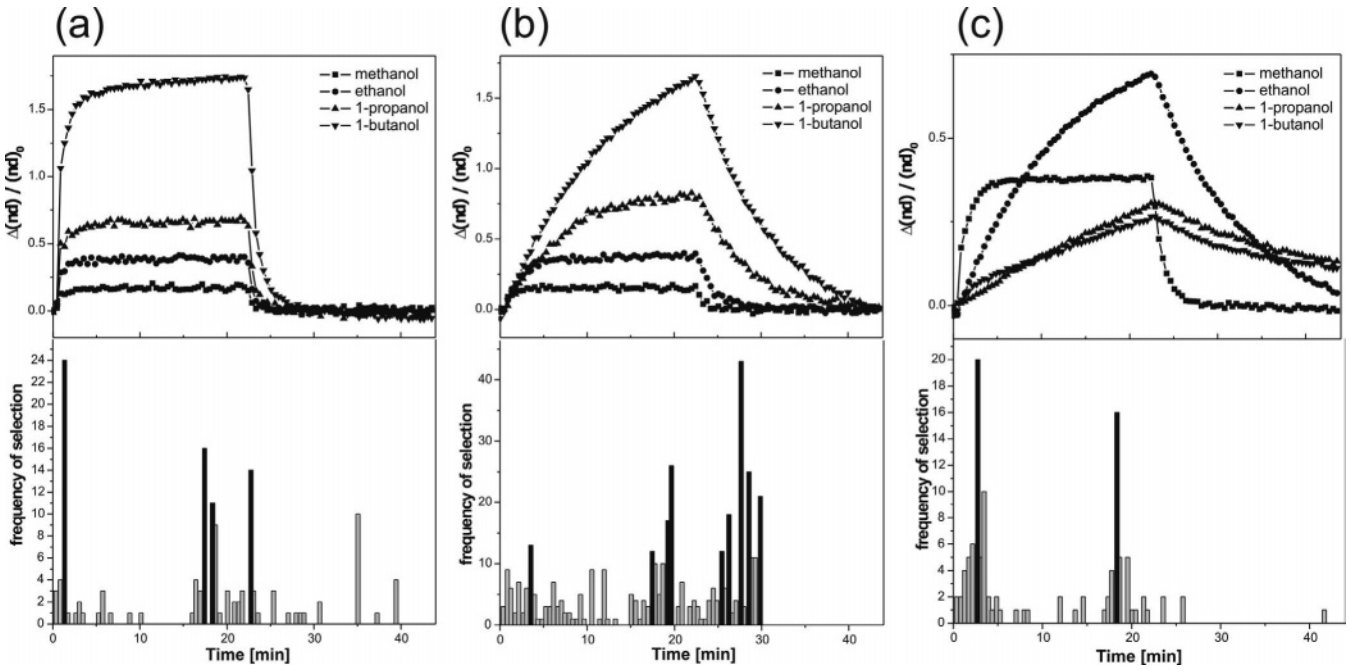

Figure 6. Importance of the various time points for HBP−OH (a), HBP−OAc (b), and PI 2566 (c) expressed as frequency of selection by the variable selection procedure.

of analyte exposure, at the end of analyte exposure (corresponds to the maximum of signal), and at the beginning of desorption of analyte are selected. These time points can be correlated with the highest differences of interaction kinetics when inspecting the sensor responses of pure analytes. In contrast to the PI 2566 sensor and the HBP−OH sensor, the importance of time points is more scattered for the HBP−OAc sensor, because the differences of interaction kinetics for the four analytes are more or less constant for the complete response curve.

These results clearly demonstrate that the variable selection procedure allows an automatic identification and selection of time points most suited for the multianalyte quantification in mixtures. On the basis of these results, an optimization of the measurement is possible, and the duration of measurements can be reduced because over long time intervals during exposure to analyte, no variables are used (only at the beginning and at the end or sorption). This should allow reduction of the measurement time during sorption and simultaneously during desorption. At the moment, a complete measurement cycle takes 45 min. Thus, the time needed to record a four-level full factorial calibration data set takes 192 h. Although this calibration has to be performed only once for a specific matrix (the sensors proved to be very stable during all measurements reported here and during many additional measurements), a significant reduction of measurement is crucial for practical applications.

An interesting point is the simulation of single-sensor setups for an assessment of the different contributions of the single sensors for the quantification of mixtures. If the temporal-resolved shapes of the sensor signals of a sensor differ enough, a single-sensor setup should be feasible. Neural networks using only the variables of one sensor were trained by the calibration data set. In Table 1, the prediction errors of the validation data are listed. Methanol and ethanol are best predicted using the PI 2566 sensor, whereas 1-propanol and 1-butanol are best predicted using the HBP−OAc sensor. The prediction errors of the HBP−OH sensor for all four alcohols are very high.

An explanation of the difference in performance of these three single sensor setups for the quantification of certain alcohols in mixture can be given on the basis of the knowledge of the interaction kinetics of the sensors with single analytes. In the case of the PI 2566 single sensor, the interaction kinetics for methanol and ethanol differ strongly, resulting in different temporal information of the sensor signal for these alcohols. Visible as low prediction error, these differences in temporal information enable the quantification of these two alcohols in mixtures. In the same way, the low prediction errors of 1-propanol and 1-butanol using the HBP−OAc single sensor can be explained, because a similar situation was found. On the other hand, the weak prediction of the two lower alcohols using this sensor clearly demonstrates the fundamental role of differences in interaction kinetics. Because the sorptions and desorptions of these alcohols occur in a similar period, the differences in interaction kinetics are not distinct. The poorest prediction of the four alcohols with a mean prediction error of 46.2% was achieved by using a HBP−OH single-sensor setup. As discussed before, differences of interaction kinetics of the sensor signals of the four alcohols can be found just at the beginning of sorption and desorption. The time resolution used for recording the sensor response is too low for a successful differentiation of all four analytes. Nevertheless, the sensor can contribute information to a sensor array by differences of the signal height, similar to a conventional sensor. Additionally, the sensor response at the beginning of sorption and desorption can be attributed to the quantification of 1-butanol.

The combination of temporal-resolved measurements of HBP−OAc and of PI 2566 should be enough for the quantification of all four analytes. Thus, only the time points of these two sensors were used for the data analysis. In Table 1, the mean prediction error and the prediction error for each alcohol are given. The

results are comparable to the prediction by all three sensitive layers using the growing artificial neural networks. The good performance of the two-sensor setup demonstrates the power of temporal-resolved measurements if appropriate sensitive layers are available.

CONCLUSIONS

The combination of temporal-resolved measurements with artificial neural networks has been proven to be a powerful tool for the quantification of multianalyte mixtures in water using a reduced number of sensors. Quaternary mixtures of methanol, ethanol, 1-propanol, and 1-butanol in water were successfully quantified using a sensor system with two hyperbranched and one microporous polymer as sensitive layers. The interaction between the polymers and the analytes was investigated using single analyte measurements. The hyperbranched polymer with acetate groups and the microporous polymer showed different sorption and desorption kinetics for all four analytes. Thus, quantifications of the four analytes were possible using temporal-resolved sensor responses of three and of only two sensors. It was shown that quantifications of quaternary mixtures are possible even with a single sensor. A feature selection based on growing neural networks confirmed the visual inspection and interpretation of single sensor responses in terms of most discriminating time intervals for each sensor.

In this work, it was demonstrated that the principle of temporal-resolved measurements for reducing the number of sensors can be extended to the aqueous phase. Hyperbranched polyesters have been introduced as suitable sensor materials for temporal-resolved measurements in aqueous phase.

Until now, temporal-resolved measurements with polymer sensors have been reported only in the gaseous phase. It was shown that the maximal heights of sensor responses for analytes of different sizes differ between the gaseous and the aqueous phases. This can be traced back to the sensor layers being swollen due to the uptake of water molecules. It was demonstrated that differences in macromolecular architecture and functional groups have a strong influence on interaction kinetics with various analytes. In conclusion, this opens the door for tailoring hyperbranched polymers for temporal-resolved measurements of different sized analytes. Hydrogen bond linkage of hyperbranched polymers with suitable functional groups can be altered by annealing the polymer layers above the glass transition temperature.[31,32] Thus, it will be possible to influence the interaction kinetics of the HBP−OH sensor. In consequence, further investigations to understand the importance of hydrogen bonds on macromolecular architecture and to assess the possibility of influencing interaction kinetics by annealing are needed.

Received for review March 13, 2005. Accepted July 8, 2005.

AC0504316